Polymer Chemistry

Accepted Manuscript

This is an *Accepted Manuscript*, which has been through the Royal Society of Chemistry peer review process and has been accepted for publication.

Accepted Manuscripts are published online shortly after acceptance, before technical editing, formatting and proof reading. Using this free service, authors can make their results available to the community, in citable form, before we publish the edited article. We will replace this *Accepted Manuscript* with the edited and formatted *Advance Article* as soon as it is available.

You can find more information about *Accepted Manuscripts* in the Information for Authors.

Please note that technical editing may introduce minor changes to the text and/or graphics, which may alter content. The journal's standard Terms & Conditions and the Ethical guidelines still apply. In no event shall the Royal Society of Chemistry be held responsible for any errors or omissions in this *Accepted Manuscript* or any consequences arising from the use of any information it contains.

ROYAL SOCIETY OF CHEMISTRY

www.rsc.org/polymers

CREATED USING THE RSC ARTICLE TEMPLATE (VER. 3.1) - SEE WWW.RSC.ORG/ELECTRONICFILES FOR DETAILS
ARTICLE TYPE www.rsc.org/xxxxxx | XXXXXXXX

Multiple Hydrogen Bonding Mediates the Formation of Multicompartment Micelles and Hierarchical Self-Assembled Structures From Pseudo A-*block*-(B-*graft*-C) Terpolymers

Yi-Chen Wu,[a,b] Bishnu Prasad Bastakoti,[b] Malay Pramanik,[b] Yusuke Yamauchi,[b] and Shiao-Wei Kuo[a,*]

Received (in XXX, XXX) Xth XXXXXXXXX 200X, Accepted Xth XXXXXXXXX 200X
First published on the web Xth XXXXXXXXX 200X
DOI: 10.1039/b000000x

In this study, we report a simple but effective method for preparing various multi-compartment micelle structures: poly(styrene-*b*–4-vinylbenzyl triazolylmethyl methylthymine) (PS-*b*-PVBT) diblock copolymers blending with the adenine-terminated poly(ethylene oxide) (A-PEO) homopolymer to obtain pseudo A-*b*-(B-*g*-C)–type terpolymers stabilized through thymine-adenine (T-A) multiple hydrogen bonding interactions between PVBT and A-PEO segments in DMF (*N*,*N*-dimethylformamide) common solvent after the addition of (H_2O or MeCN) selective solvent. Transmission electron microscopy revealed several different multi-compartment micelle structures—raspberry-like spheres, core–shell–corona spheres, core–shell–corona cylinders, nanostructured vesicles, onion-like structures, segmented worm–like cylinders, and woodlouse-like structures—upon varying the molecular weight of the PS-*b*-PVBT block segments and the concentration of the selective solvent. Thus, we could induce changes in the multi-compartment micelle structures, similar to those of ABC miktoarm star terpolymers, through simple blending of PS-*b*-PVBT block copolymers with an A-PEO homopolymer.

Introduction

Block copolymers can lead to the formation of self-assembly micelle structures with an insoluble hydrophobic block core surrounded by a hydrophilic block shell since such systems can display fascinating nanostructures (e.g., spherical, cylindrical, and vesicular micelles) of high stability. They possess much interesting for the delivery of drugs, genes and proteins.[1,2] The hydrophilic shell can stabilize the hydrophobic core as an interface between the hydrophobic region and aqueous phase. In addition, the hydrophobic block core can be as a carrier compartment to accommodate predominately hydrophobic drugs.[3]

The self-assembly of more-complex macromolecules (e.g., ABC linear triblock terpolymers) into multi-compartment micelles has also attracted much interest in recent years.[4–9] With an appropriate selective solvent, the three linear individual block segments of an ABC linear triblock terpolymer can undergo core–shell–corona compartment aggregation.[4] In addition, the ability to form of ABC miktoarm star terpolymers in selective solvent for one block segment is quite an attractive proposition. Here, C usually represents the hydrophilic block segment and A and B represent different hydrophobic blocks.[10–14] The overall size and shape of the multi-compartment micelles are strongly dependent on the internal arrangement of hydrophobic components formed between the A and B block segments. A variety of multi-compartment micelles have been prepared, including raspberry-like, hamburger-like, segmented worm–like, and nanostructured vesicle micelles, through changes in the relative block segment ratios and architectures.[4] The advantage to using ABC miktoarm star terpolymers is suppressed formation of core–shell–corona structures, because these three block segments should meet along a curve in space among the three interfacial energies and the relative block lengths.[4] In addition to ABC triblock terpolymers, A-*block*-(B-*graft*-C) or dendritic-amphiphilic copolymers have also been used to fabricate hierarchical multi-compartment micelles.[15]

Nevertheless, the syntheses of ABC linear triblock copolymers, ABC miktoarm star terpolymers, and A-*block*-(B-*graft*-C) terpolymers could be difficult and time-consuming. Another approach for the preparation of multi-compartment micelles is through blending of two or more different block copolymers. The blending the polymers in various ratios is a relatively simple method for systematically varying micelle structures without the need for tedious syntheses of multi-block copolymers of various compositions.[16–18] For example, Webber *et al*. reported core–shell–corona spherical micelles through the blending of A-*b*-B and B-*b*-C diblock copolymers; their B block segment displayed pH-dependent water-solubility.[19] Zhu *et al*. described the transformation of spherical core–shell–corona micelles to cylindrical core micelles upon blending amphiphilic A-*b*-B copolymers with several different hydrophobic B-*b*-C diblock copolymers.[20] Lodge *et al*. reported various multi-compartment micelles that formed when blending A-*b*-B copolymers with star-like ABC triblock copolymers.[21] Pochan *et al*. blended ACB and ABD triblock terpolymers to form multi-compartment micelle structures.[22] As mentioned above,[19–22] these multi-compartment micelles are usually produced by blending diblock or triblock copolymers. Because the syntheses of block copolymers are generally difficult and time-consuming, by using the noncovalently connected micelles (NCCMs) to prepare self-assembly micelle is attractive from complementary homopolymer pairs.[23-28] Jiang *et al*. reported NCCMs from a "block copolymer–free" method using complementary homopolymers pairs.[23] Terminally functionalized homopolymers blended with side-chain–functionalized homopolymers or copolymers form "graft-like"

[a]Department of Materials and Optoelectronic Science, Center for Nanoscience and Nanotechnology, National Sun Yat-Sen University, Kaohsiung, 804, Taiwan
E-mail:kuosw@faculty.nsysu.edu.tw
[b]World Premier International (WPI) Research Center for Materials Nanoarchitectonics (MANA), National Institute for Materials Science (NIMS), 1-1 Namiki, Tsukuba, Japan
E-mail: Yamauchi.Yusuke@nims.go.jp

Polymer Chemistry Accepted Manuscript

copolymers stabilized through hydrogen bonding in common solvent. For example, carboxyl-terminated polystyrene (PS)

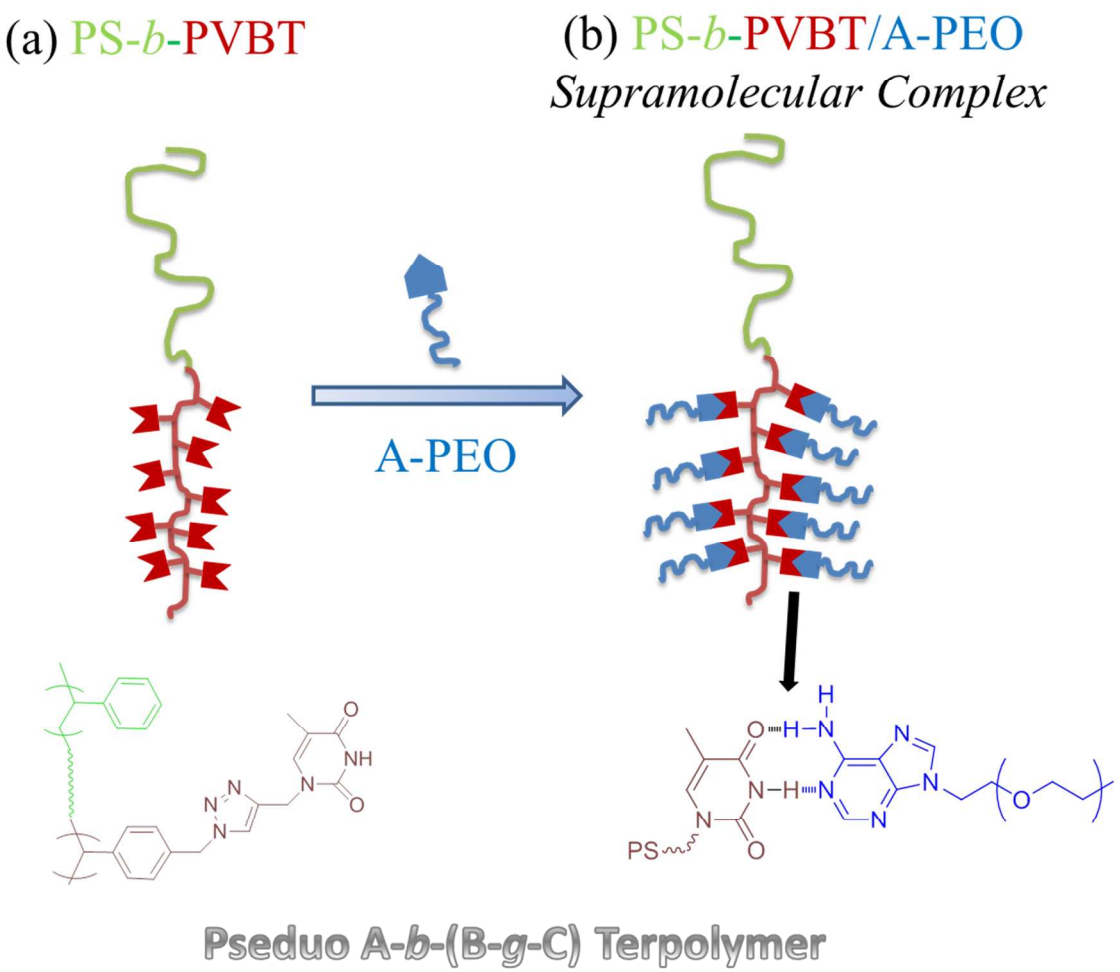

Scheme 1: Cartoon representations of (a) PS-*b*-PVBT and (b) the supramolecular complex PS-*b*-PVBT/A-PEO, with a chemical structure of the interaction between the T and A units.

oligomers interacting with poly(4-vinylpyridine) (P4VP), stabilized through COOH···pyridine hydrogen bonding.[25]

In this study, we introduce the very simple route for the preparation of various multi-compartment micelles: blending hydrophobic A-*b*-B diblock copolymers with terminally functionalized hydrophilic C homopolymers (i.e., through blending of only the diblock copolymer with the homopolymer). We synthesized poly(styrene-*b*-4-vinylbenzyl triazolylmethyl methylthymine) (PS-*b*-PVBT) by using nitroxide-mediated radical polymerization to prepare the poly(styrene-*b*-4-vinylbenzyl azide) (PS-*b*-PVBN$_3$), followed by click chemistry with propargyl-thymine (PT) to obtain the thymine (T)-containing PS block copolymers (**Scheme S1**). We employed an adenine (A)-terminated poly(ethylene oxide) (A-PEO) homopolymer (**Scheme S2**) to induce bio-inspired DNA-like (between the A and T units) multiple hydrogen bonds. The resulting PS-*b*-PVBT/A-PEO supramolecular complexes were stabilized through these strong noncovalent interactions (**Scheme 1**), behaving as pseudo A-*b*-(B-*g*-C) terpolymers. To prepare the multi-compartment micelles, we first dissolved the PS-*b*-PVBT/A-PEO supramolecular complex in DMF (*N*,*N*-dimethylformamide) common solvent and then added two different selective solvents of water and MeCN. By varying the molecular weights of the PS-*b*-PVBT block segments and the contents of the selective solvents, we obtained a variety of multi-compartment micelles: raspberry-like spheres, core–shell–corona spheres, core–shell–corona cylinders, nanostructured vesicles, onion structures, and segmented worm–like cylinders, and woodlouse-like structures. Through simple blending of the A-PEO homopolymer and the PS-*b*-PVBT block copolymers, we could observe multi-compartment micelles structures similar to those formed by ABC miktoarm star terpolymers.

Experimental

Materials

Styrene and 4-vinylbenzyl chloride (VBC) are obtained from Aldrich, passed through the alumina column and then vacuum-distilled from CaH_2 under reduced pressure prior to use. TEMPO-OH initiator was synthesized as described previously.[29] PS-*b*-PVBT copolymers with different lengths of their chains containing T units, were synthesized through nitroxide-mediated radical polymerization, to yield PS-*b*-PVBN$_3$, followed by click chemistry with PT.[30–32] A-PEO was synthesized through the reaction of monomethoxy-poly(ethylene poly(ethylene oxide) with TsCl (to form PEO-TsCl) and a subsequent reaction with adenine and K_2CO_3 in DMF, as described previously.[33]

Polymer Chemistry Accepted Manuscript

This journal is © The Royal Society of Chemistry [year]

Table 1: Molecular weights and thermal properties of PS-*b*-PVBT diblock copolymers used in this study

Sample[a]	PS (M_n)[a]	PVBT (M_n)[a]	PDI[b]	T_g (°C)[c]
PS_{67}-*b*-$PVBT_{16}$	7100	8840	1.17	104/157
PS_{87}-*b*-$PVBT_{22}$	9000	7400	1.20	109/165

[a]: Determined from ^{1}H NMR spectra. [b]: Determined from GPC analysis. [c]: Determined from DSC analysis.

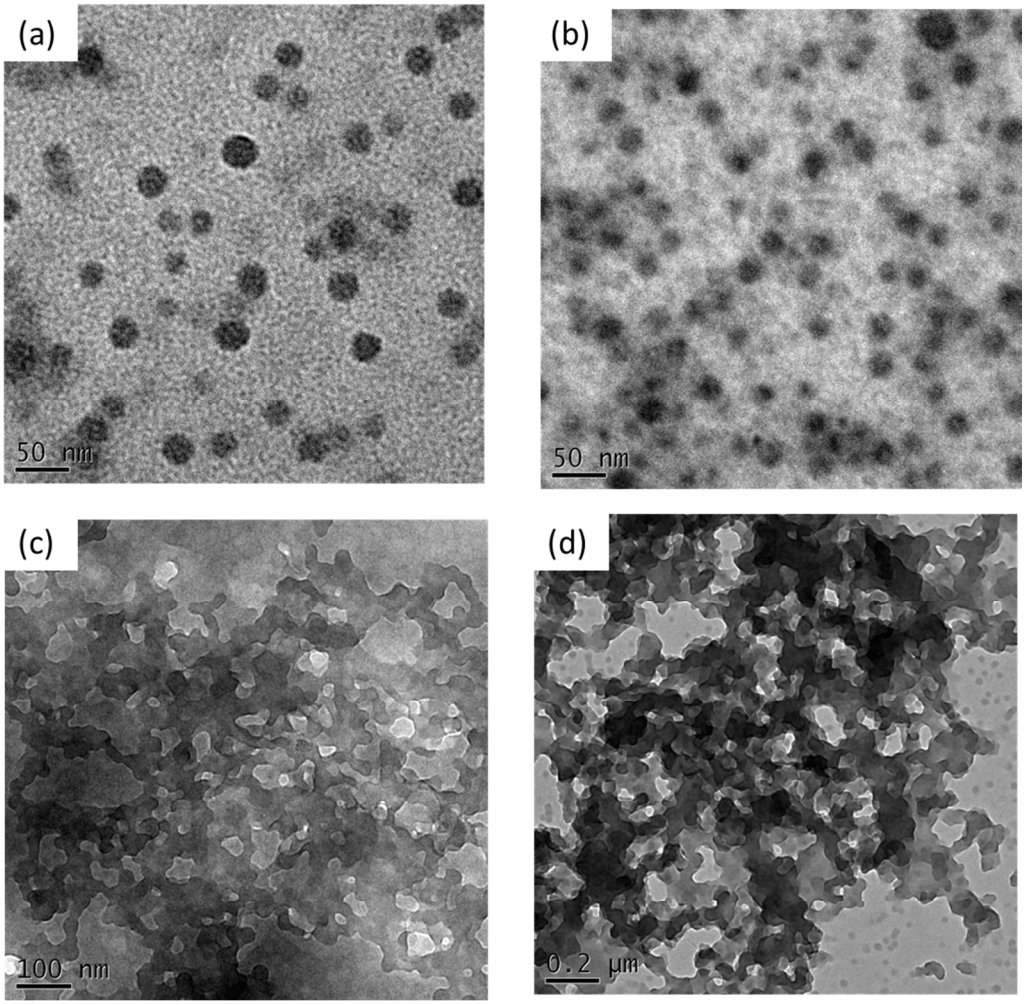

Figure 1: TEM images of the PS_{87}-*b*-$PVBT_{22}$/A-PEO supramolecular complexes formed in DMF/H_2O solutions containing various water contents of (a) 1, (b) 2, (c) 5, and (d) 10 wt%.

Micelle Structures From PS-*b*-PVBT/A-PEO Supramolecular Complexes

A PS-*b*-PVBT/A-PEO supramolecular complex was dissolved in DMF (5 mg/mL), which is a good solvent for all of the segments (PS, PVBT, and A-PEO). A volume of H_2O or MeCN was added gradually into the DMF solution of the blend, with stirring (H_2O and MeCN are non-solvents for the PS blocks). The formation of micelles was determined by the turbidity appearance in the solution. The addition of H_2O or MeCN was continued until the desired concentration was reached; the DMF was then removed through dialysis against toluene.

Characterization

^{1}H and ^{13}C NMR spectra were measured by using the Varian Unity Inova 500 spectrometer from solutions in $CDCl_3$ and d_6-DMSO. Molecular weights and polydispersity (PDI) were determined by using gel permeation chromatography (GPC) at 80 °C with a 410 differential refractometer, and three Ultrastyragel columns (100, 500, and 103 Å) connected in series; DMF was the eluent; the flow rate was 1 mL/min. PS standards was used for the molecular weight calibration curve. The hydrodynamic diameters of the micelles were measured using Brookhaven 90Plus apparatus (Brookhaven Instruments, USA) of dynamic light scattering (DLS) at 25 °C and a He–Ne laser (power: 35 mW; wavelength: 632.8 nm) at an angle of detection of 90°. All samples were measured more than five times. Small-angle X-ray scattering (SAXS) analyses were recorded by using the BL17A1 wiggler beamline of the National Synchrotron Radiation Research Center (NSRRC), Taiwan. An X-ray beam having a diameter of 0.5 mm and a wavelength (λ) of 1.1273 $Å^{-1}$ was used for the SAXS

Polymer Chemistry Accepted Manuscript

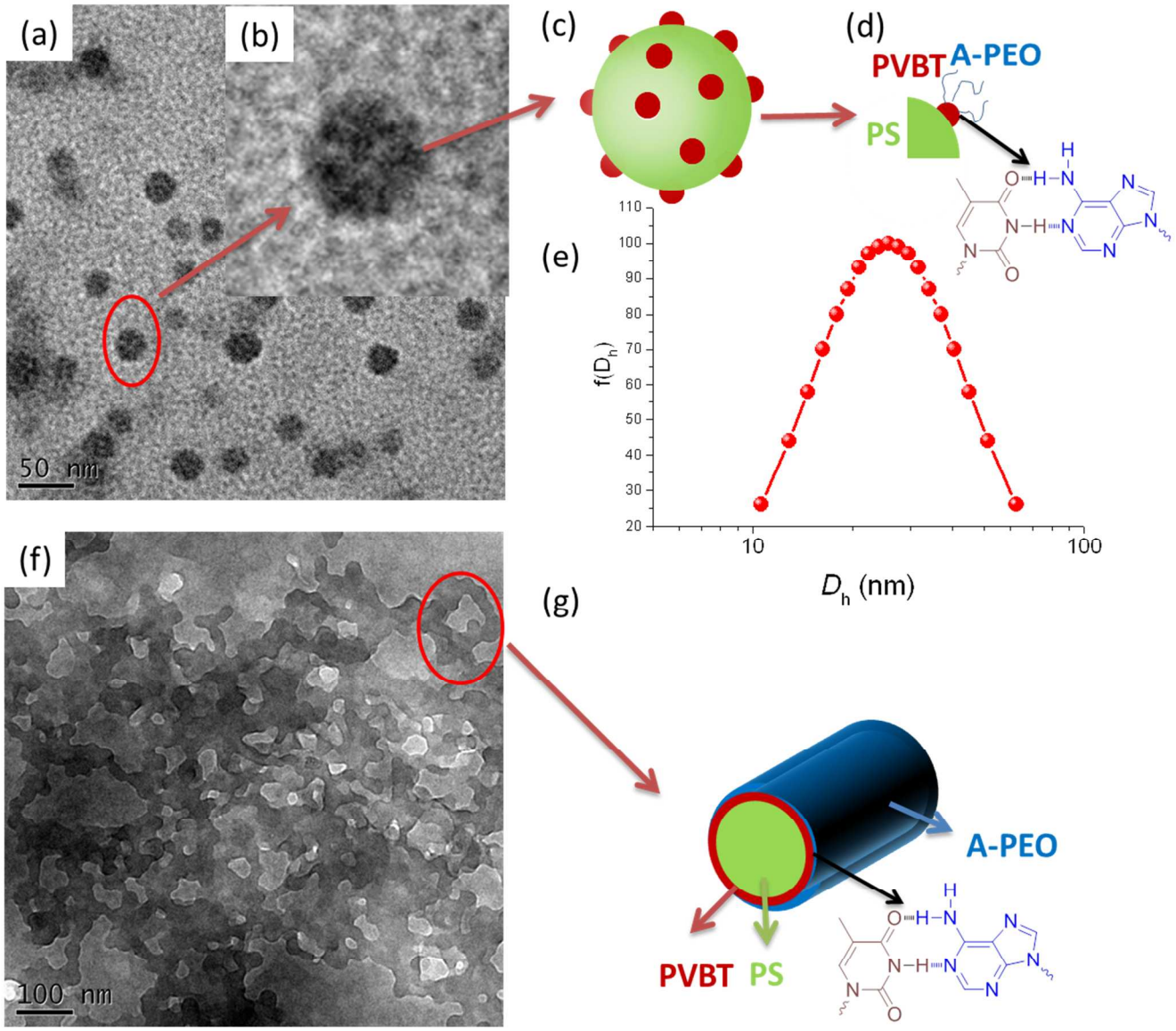

Figure 2: (a-b) TEM images of PS_{87}-*b*-$PVBT_{22}$/A-PEO supramolecular complex formed in DMF/H_2O solution at 1 wt% water content. Inset: Magnified image. (c-d) Schematic representation of the raspberry-like spheres in (a). (e) Size-distributions of the micelles by DLS. (f) TEM image of the PS_{87}-*b*-$PVBT_{22}$/A-PEO supramolecular complex formed in DMF/H_2O solution at 5 wt% water content. (g) Schematic representation of a possible structure for the core–shell–corona cylinder morphology observed in the TEM image in (f).

measurements. Wide-angle X-ray diffraction (WAXD) data were determined using the NANOSTAR U X-ray scattering system (Bruker AXS, Karlsruhe, Germany) and Cu Kα radiation (30 W, 50 kV, 600 μA). Transmission electron microscopy (TEM) was performed using the JEOL 2100 microscope (Japan) operated at 200 kV. To observe the micelle structures under TEM and to maintain the original morphology as in the solution, a small amount of excess water solution was quenched to quickly vitrify the PS and PVBT blocks into their glass state and then the micelles were placed onto Cu grids, which was coated with carbon-supporting films. The micelles were followed by staining with I_2 vapor through exposure to determine the PVBT/A-PEO complexes since I_2 is a preferential staining agent for thymine (T) and adenine (A) units and thus, the domains of PVBT/A complex appeared dark, and the domains of PS and PEO appeared bright in the TEM images.

Results and Discussion

Self-Assembly of PS-b-PVBT Diblock Copolymers in the Bulk State

Table 1 summarizes the thermal properties and molecular weights, as determined through GPC (**Figure S1**), ^{1}H NMR spectroscopy (**Figure S2**), and DSC analyses, of these two PS-*b*-PVBT diblock copolymers used in this study. **Figures S3(a)** and **S3(b)** display the SAXS analysis data of pure PS_{67}-*b*-$PVBT_{16}$ and PS_{87}-*b*-$PVBT_{22}$. These two pure diblock copolymers possessed long-range-ordered lamellar microdomain structures, due to the high-order scattering peaks at the scattering vectors q with (q/q_m = 1, 2, 3, 4, and 5) relative

Polymer Chemistry Accepted Manuscript

This journal is © The Royal Society of Chemistry [year]

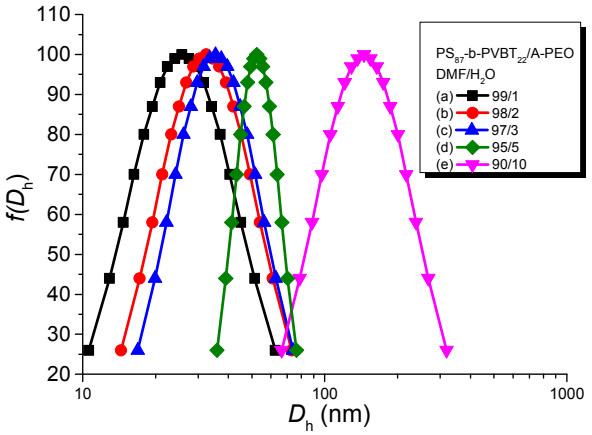

Figure 3: DLS data for the PS_{87}-*b*-$PVBT_{22}$/A-PEO supramolecular complexes formed in DMF/H_2O solutions at various water contents of (a) 1, (b) 2, (c) 3, (d) 5, and (d) 10 wt%.

to the first order scattering peaks. TEM images [**Figures S3(c)** and **S3(d)**] confirmed these structures. The two SAXS peaks appeared at positions of multiple q of 0.041 and 0.025 $Å^{-1}$ indicate lamellar phases having long periods of 15.3 and 25.1 nm based on the first peak position ($2\pi/q$), for pure PS_{67}-*b*-$PVBT_{16}$ and PS_{87}-*b*-$PVBT_{22}$, respectively. The result is reasonable: the pure PS_{87}-*b*-$PVBT_{22}$ diblock copolymer should exhibit larger alternating lamellar domains in the bulk state because its molecular weight is higher than that of PS_{67}-*b*-$PVBT_{16}$, while their volume fractions of PS blocks are similar ($f^{v}_{ps} = 0.64$).[30]

Self-Assembly of PS-b-PVBT/A-PEO Supramolecular Complexes in DMF/H_2O Solution

Pure PS-*b*-PVBT diblock copolymers are not able to self-assemble in the selective solvent of a water solution because both blocks are hydrophobic. In contrast, the A-PEO homopolymer is water-soluble and hydrophilic; therefore, we expected the supramolecular complex of PS-*b*-PVBT/A-PEO is able to form self-assembly micelles in the water selective solvent. The self-assembled structures from spherical micelles to cylinders, vesicles, and lamellae can be mediated by changing the amounts of selective solvent to shift the micro-phase separation of block copolymers.[34,35] We first dissolved a PS-*b*-PVBT/A-PEO supramolecular complex in DMF common solvent, which is a good solvent for PS, PVBT and A-PEO segments. Then, we added the selective solvent of water or MeCN, the poor solvent for PS and PVBT blocks very slowly. Cheng *et al*. have reported that the micellization and the morphological transition of PS-*b*-PEO block copolymer in both DMF/H_2O and DMF/MeCN systems, which was strongly dependent on the water and MeCN contents in these studies.[36,37] As a result, we also chose these two different selective solvents of H_2O and MeCN to investigate their self-assembly effects of our PS-*b*-PVBT/A-PEO supramolecular complexes in this study.

Figure 1 presents TEM images of a PS_{87}-*b*-$PVBT_{22}$/A-PEO supramolecular complex where the T/A ratio was 1:1 in DMF/H_2O solutions containing various H_2O ratios. We observed a raspberry-like sphere (or sphere-on-sphere) structure [**Figure 1(a)**] at a relatively low concentration of water (1 wt%). Diblock copolymers always show spherical micelles having a hydrophobic core and a hydrophilic shell after the addition of water.[38] In this study, the hydrophilic A-PEO coronas imparted solubility to the spherical micelles in water, while their hydrophobic PS and PVBT block segments should be thermodynamic immiscible (Figure S3), resulting in strong micro-phase separation in the bulk state. Therefore, we observed raspberry-like ("sphere-on-sphere") spheres with nearly identical sizes (ca. 20–30 nm) for the multi-compartment micelles in **Figures 2(a)** and **2(b)**, as confirmed through DLS [**Figure 2(e)**]. This raspberry-like sphere is close to the diameter of full contour length of the chain. A schematic representation of the possible morphology is displayed in **Figure 2(c)**, with the interface between PVBT and A-PEO connected through T and A multiple hydrogen bonding interactions [**Figure 2(d)**]. **Figure 1(b)** reveals that spherical micelle morphologies also formed at a 2 wt% water concentration. At concentrations of 5 and 10 wt%, however, the morphologies changed to long, wormlike cylinders [several micrometers; **Figures 2(c)** and **2(d)**]. Because of the immiscibility of the PS and PVBT block segments, these wormlike structures may have possessed core–shell–corona cylinder structures, as displayed in **Figures 2(f)** and **2(g)**. **Figure 3** summarizes the hydrodynamic diameters through DLS data of the PS_{87}-*b*-$PVBT_{22}$/A-PEO supramolecular complexes formed in the DMF/water system. The addition of 1 wt% water led to polymer aggregate sizes ca. 20–30 nm; this range is consistent with the TEM images. Further increasing the water content to 2 or 3 wt% caused the sizes of micelles to increase accordingly, as expected. At 5 or 10 wt% water content, cylindrical structures were formed, resulting in values of D_h larger than those of the spherical structures.

To observe the structures formed at water contents higher than 10 wt%, we examined the PS_{67}-*b*-$PVBT_{16}$/A-PEO supramolecular complex in the DMF/water system; the lower molecular weight of the PS block decreased the core-chain stretching and inhibited precipitation in the DMF/water system at elevated water contents. **Figure 4** presents TEM images of the PS_{67}-*b*-$PVBT_{16}$/A-PEO supramolecular complexes formed at t a T/A ratio of 1:1 in DMF/H_2O solutions of various water ratios. The vesicle structures were clearly observed for all of the high-water-content systems (>10 wt%). As revealed in **Figures 4(a)–4(d)**, vesicles with bilayer structures were formed; **Figure 5(a)** displays an enlarged image. Almost-monodisperse bilayer vesicles were evident at 10 and 15 wt% water contents, with the sizes of the vesicle micelles determined from the TEM images, which are close to the hydrodynamic diameters based on the DLS data [ca. 150–200 nm; **Figure 5(c)**]. Vesicle structures can form readily with low bilayer bending elasticity and high surface tension as revealed in **Figures 5(b)** and **5(e)**. When the water content was 10 or 15 wt%, the conformations of the PS and PVBT blocks were extended relative to those at water contents below 10 wt%, allowing the block copolymer chains to pack in parallel to micelles having layer lamellae structures. Ultimately, the structures formed vesicles to minimize the surface energy in solution. We suspect that the inner- and outer-layer polymer chains of the vesicles were located from the A-PEO homopolymer segment, as displayed in **Figure 5(b)**. PS and PVBT block segments are immiscible, and PVBT can undergo complementary multiple hydrogen bonding with A-PEO. Therefore, the resulting vesicular complex is composed of an outer layer of PEO segments (majority), a trilayer of a PVBT/PS/PVBT microphase-separated wall (ca. 30 nm, double size of lamellar thickness based on SAXS analyses in Figure S3), and an inner layer of PEO segments (majority). Further increasing the water content

Polymer Chemistry Accepted Manuscript

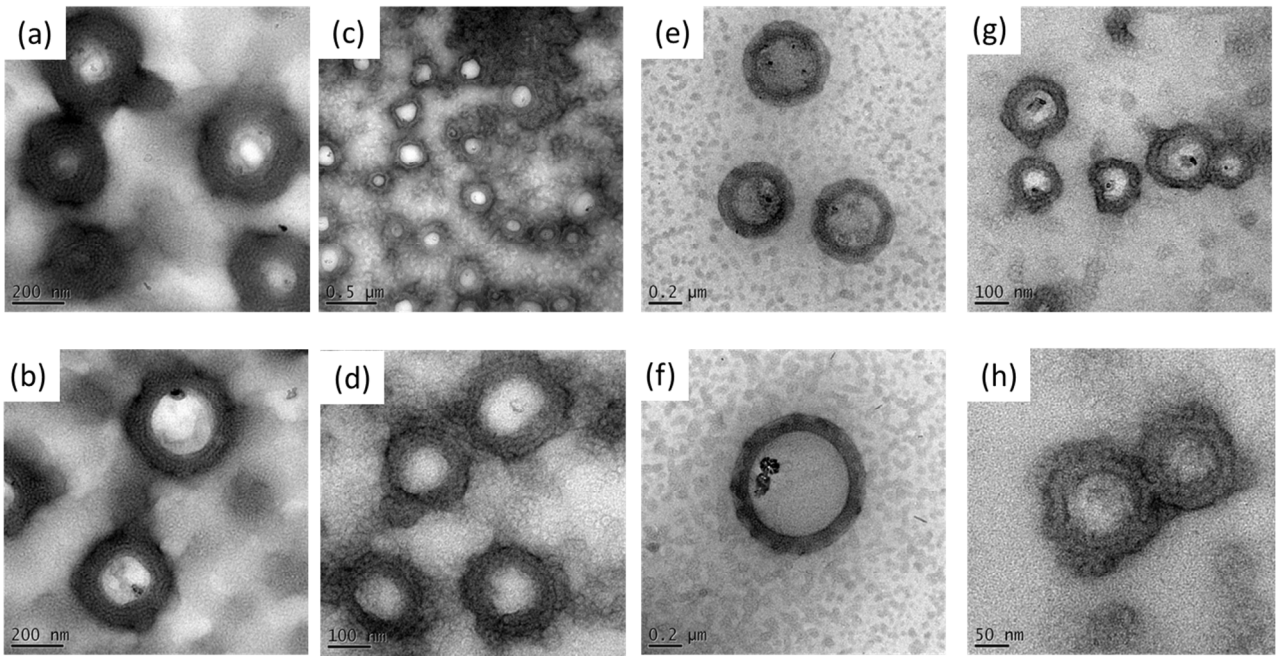

Figure 4: TEM images of the PS_{67}-*b*-$PVBT_{16}$/A-PEO supramolecular complexes formed in DMF/H_2O solutions at various water contents of (a, b) 10, (c, d) 15, (e, f) 25, and (g, h) 35 wt%.

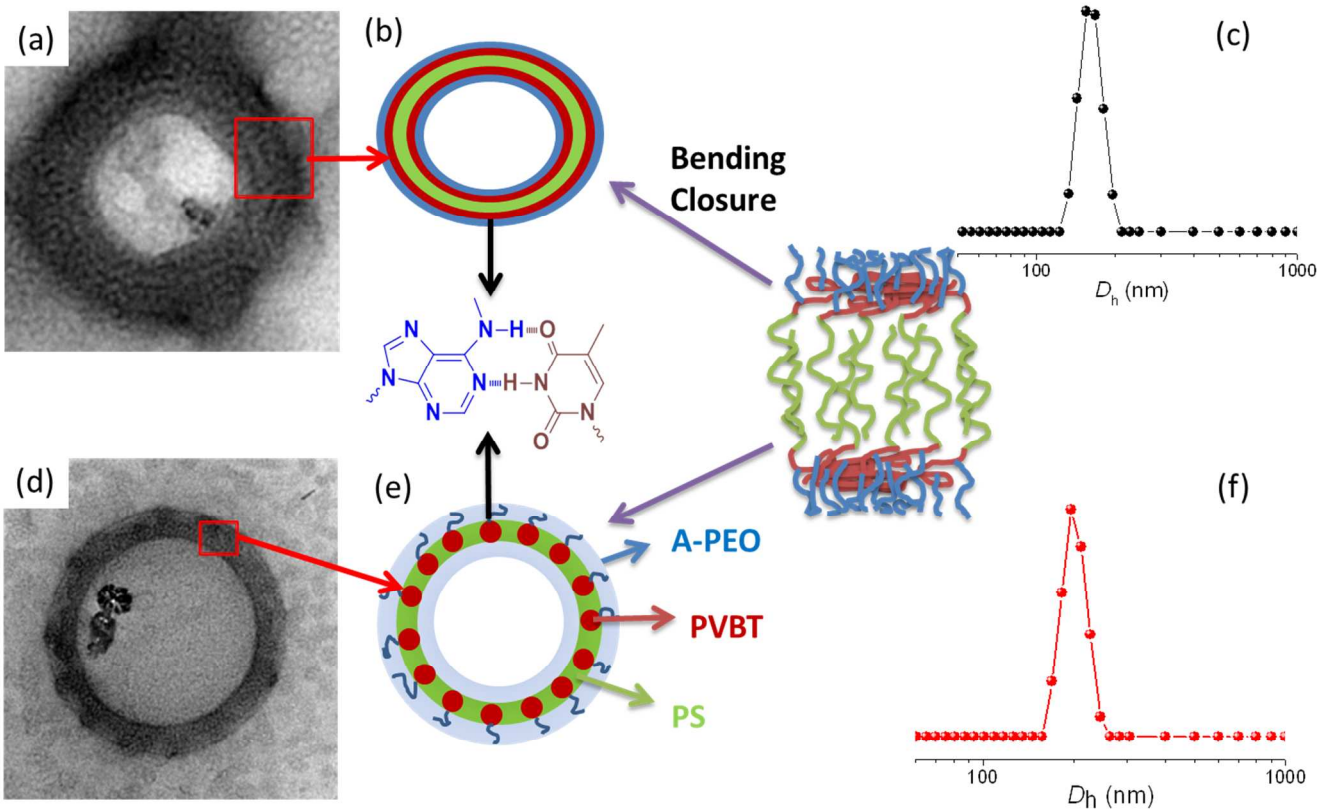

Figure 5: (a) Expanded TEM images of the PS_{67}-*b*-$PVBT_{16}$/A-PEO supramolecular complex formed in DMF/H_2O solution at 10 wt% water content. (b) Schematic representation of the possible layer-vesicle structure observed in the TEM image in (a). (c) Size-distributions of the micelles by using DLS. (d) TEM image of the PS_{67}-*b*-$PVBT_{16}$/A-PEO supramolecular complex formed in DMF/ H_2O solution at 25 wt% water content. (e) Schematic representation of the possible in-plane layer vesicle structure observed in (d). (f) Size-distributions of the micelles by using DLS, corresponding to the TEM image in (d).

Polymer Chemistry Accepted Manuscript

This journal is © The Royal Society of Chemistry [year]

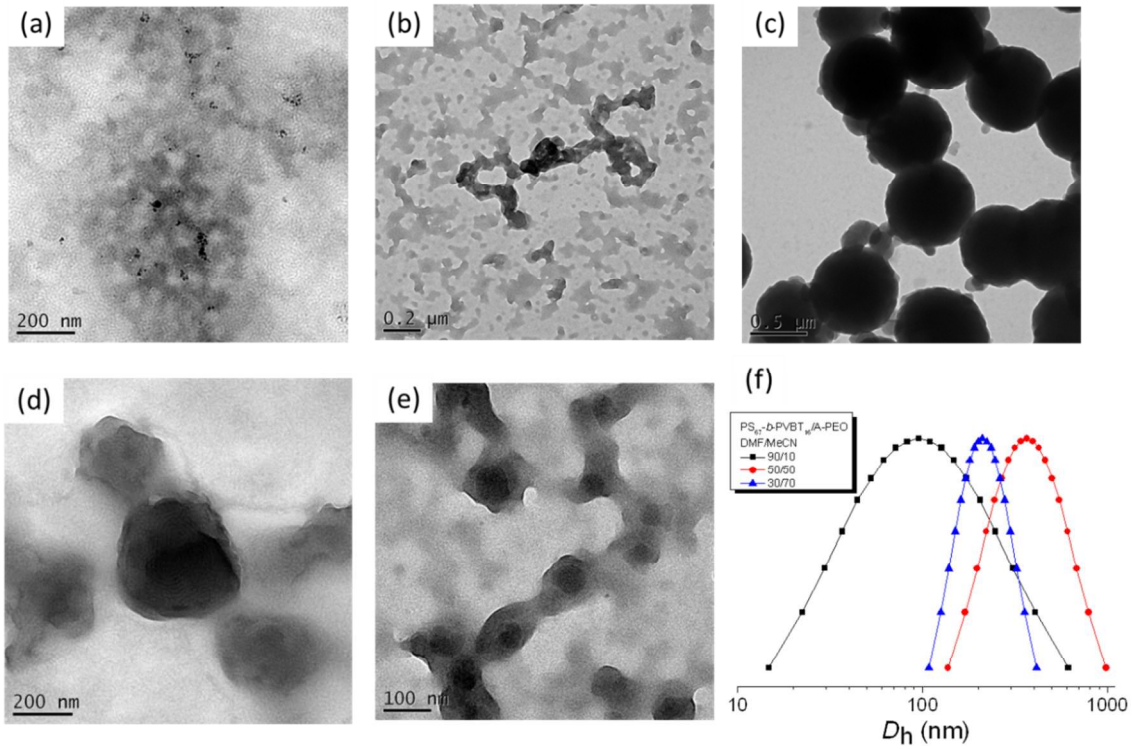

Figure 6: (a–e) TEM images of the PS_{67}-*b*-$PVBT_{16}$/A-PEO supramolecular complexes formed in DMF/MeCN solution at various MeCN contents of (a) 10, (b) 30, (c) 40, (d) 50, and (e) 70 wt%. (f) Corresponding size-distributions of the micelles by using DLS.

to 25 or 35 wt% also led to the observation of the vesicle micelles, as revealed in **Figures 4(e)–4(g)**. The vesicles were formed among in-plane bilayer structures;[4,39] **Figure 5(d)** displays an expanded image. The sizes of the vesicle micelles increased to 200–250 nm compared with relative lower water contents (10–15 wt%) by DLS data as shown in **Figure 5(f)**. Here, the wall thickness of vesicle is ca. 30 nm, which is close to previous study of vesicle structure by PS-*b*-PEO diblock copolymer in DMF/H_2O system.[36] As further increasing the water content, the PS chain mobility in the core decreased and the PS and PVBT block segments underwent multi-layer microphase separation, as presented in **Figure 5(e)**, to further minimize the free energy. Thus, water-insoluble and hydrophobic PS-*b*-PVBT diblock copolymers can readily undergo self-assembly to form multi-compartment micelles upon simple blending with a water-soluble A-PEO homopolymer, stabilized by multiple hydrogen bonding interactions between the PVBT and A-PEO block segments, in DMF/H_2O solution.

Self-Assembly of Micellar Structures From PS-b-PVBT/A-PEO Supramolecular Complexes in DMF/MeCN Solution

Figure 6 presents TEM images of the PS_{67}-*b*-$PVBT_{16}$/A-PEO supramolecular complexes formed at a T/A ratio of 1:1 in DMF/MeCN solution at various MeCN contents. Only spherical micelles were formed, regardless of the MeCN concentration. These spheres had sizes of approximately 100–200 nm at MeCN contents of 10 and 30 wt%, which is consistent with the DLS data in **Figure 6(e)** (black line). Further increasing the MeCN content to 50 wt% resulted in spheres of near-uniform size (ca. 400–500 nm), as confirmed from the DLS data in **Figure 6(e)** (red line). These spherical nanoparticles possess uniform size (ca. 150–200 nm) at the highest MeCN content (70 wt%), as confirmed from the DLS data in **Figure 6(e)** (blue line). The sizes determined from the TEM images were generally smaller than DLS measurement because TEM sample preparation was generally unavoidably leading to chain-collapse and micelle-shrinkage during evaporation of the micelle particles. The different morphological transition of the PS_{67}-*b*-$PVBT_{16}$/A-PEO supramolecular complexes in the DMF/H_2O and DMF/MeCN systems was because of the different PS–solvent interaction parameters (χ). The H_2O is a much poorer solvent than MeCN for PS segment since the $\chi_{PS-water}$ value is ca. nine times higher than the value of $\chi_{PS-MeCN}$.[36,37] The interfacial free energy increase is able to increase the micelle size and then increase the stretching of the PS blocks in the cores, resulting in the spheres readily changing to form cylinders in the DMF/H_2O system to minimize the free energy. This morphological change was not observed for the PS_{67}-*b*-$PVBT_{16}$/A-PEO supramolecular complexes in the DMF/MeCN system because of the relatively low value of $\chi_{PS-MeCN}$. The larger selective solvent content is necessary to change the interfacial free energy at certain critical point; however, in this study we could not determine this value, even at 70 wt% MeCN content.[40] To observe the morphological change in DMF/MeCN system, we turned to PS_{87}-*b*-$PVBT_{22}$/A-PEO supramolecular complex in the DMF/MeCN system because the higher molecular weight of the PS block would presumably increase the core-chain stretching and the interfacial tension between the solvent and the micellar core. As a result, we anticipated the possibility of observing the morphological change in the DMF/MeCN system.

Figure 7 displays TEM images of the PS_{87}-*b*-$PVBT_{22}$/A-PEO supramolecular complexes formed when the T/A ratio was 1:1 in DMF/MeCN solutions at various MeCN contents. **Figures 7(a)–7(c)** reveal clear core–shell–corona spherical micelles at a MeCN content of 10 wt%; **Figures 8(a)** and **8(b)** present expanded images. The sizes of these core–shell–corona

Polymer Chemistry Accepted Manuscript

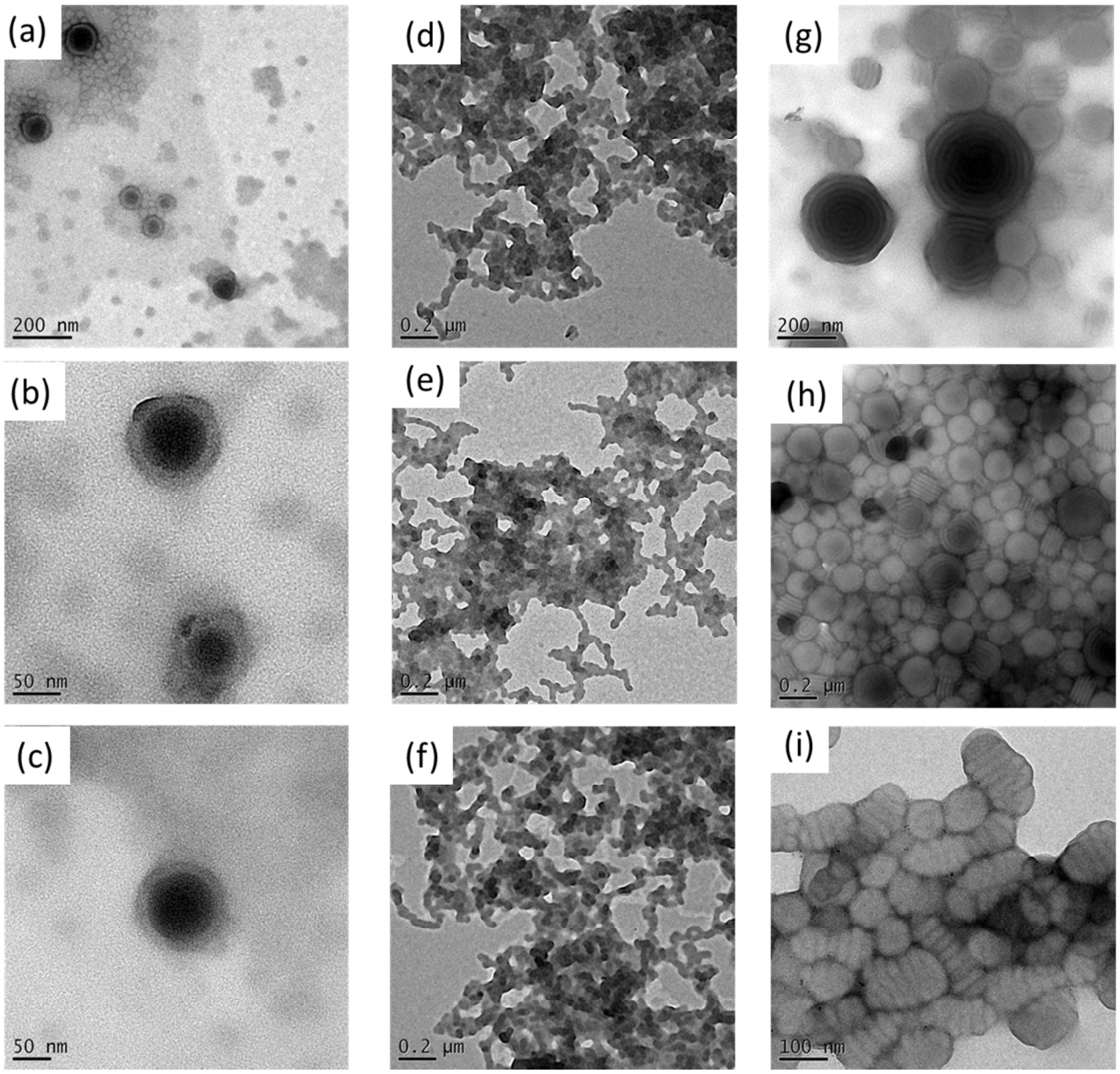

Figure 7: TEM images of the PS_{87}-*b*-$PVBT_{22}$/A-PEO supramolecular complexes formed in DMF/MeCN solution at various MeCN contents of (a–c) 10, (d–f) 30, and (g–i) 70 wt%.

spherical micelles, determined from the TEM image, were approximately 20–40 nm, consistent with the values from the DLS data in **Figure 8(d)**. From the combination of TEM images in **Figures 8(a)** and **8(b)**, all of the core–shell–corona spherical micelles featured dense dark cores (PS majority), surrounded by less-dense shells (PVBT majority), and a relatively clear boundary; the black ring in **Figure 8(a)** arises from the presence of complementary T···A multiple hydrogen bonds in the PVBT/A-PEO complex, because I_2 will stain the A units, as displayed in **Figure 8(c)**. Further increasing the MeCN content to 30 wt%, we observed clear cylinder structures [**Figures 8(d)–8(f)**] and, thus, values of D_h larger than those for the spherical structure in **Figure 8(g)**. These wormlike structures may be similar to those formed in the DMF/H_2O system, with a core–shell–corona cylinder structure, as presented in **Figure 8(f)**. The structure of the PS_{87}-*b*-$PVBT_{22}$/A-PEO supramolecular complex was quite different from that of the PS_{67}-*b*-$PVBT_{22}$/A-PEO supramolecular complex at a MeCN content of 30 wt%. The higher molecular weight of the PS block would increase the core-chain stretching and the interfacial tension between the solvent and the micellar core; thus, the spheres would change to cylinder structures at the same MeCN content to minimize the free energy as a result of decreasing the stretching penalty of the PS chains. More interestingly, upon increasing the MeCN content further, to 70 wt%, we observed regular multi-lamellar spherical structures (onion structures) and segmented worm–like structures (woodlouse structures) in **Figures 7(g)–7(i)**. These spherical and segmented worm–like structures had sizes mostly in the range 150–300 nm, as confirmed by the DLS data in **Figure 9(f)**. These onion-like spheres were in the form of a compact multi-lamella vesicular structure.[41–43] Onion-like microspheres

Polymer Chemistry Accepted Manuscript

This journal is © The Royal Society of Chemistry [year]

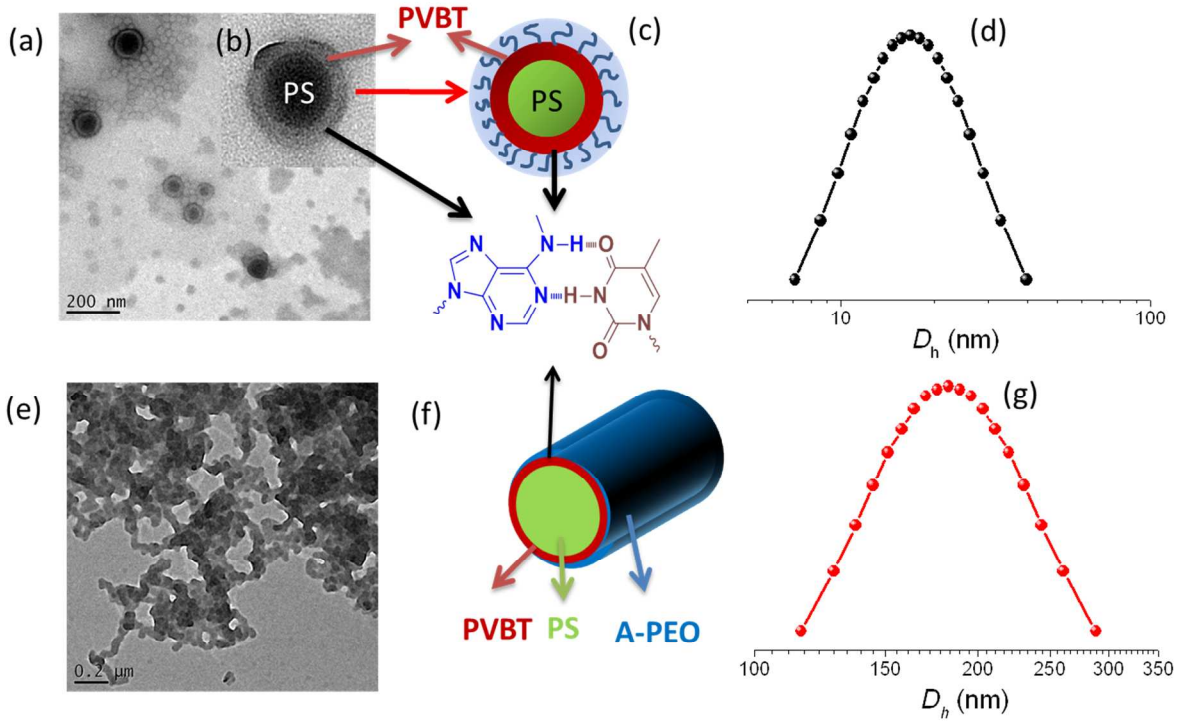

Figure 8: (a, b) Expanded TEM images of the PS_{87}-*b*-$PVBT_{22}$/A-PEO supramolecular complex formed in DMF/MeCN solution at a MeCN content of 10 wt%. (c) Schematic representation of the possible core–shell–corona sphere morphology observed in the TEM image in (b). (d) Size-distributions of the micelle by using DLS, corresponding to the TEM image in (a). (e) TEM image of the PS_{87}-*b*-$PVBT_{22}$/A-PEO supramolecular complex formed in DMF/MeCN solution at a MeCN content of 30 wt%. (f) Schematic representation of the possible core–shell–corona cylinder morphology observed in the TEM image in (e). (g) Size-distributions of the micelles by using DLS, corresponding to the TEM image in (e).

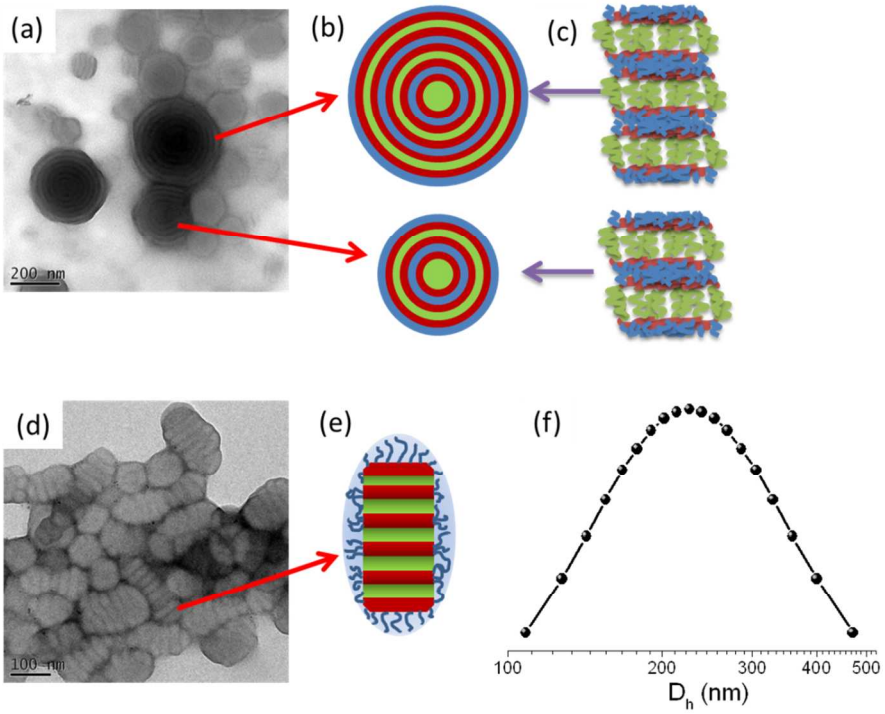

Figure 9: (a, d) TEM images of the PS_{87}-*b*-$PVBT_{22}$/A-PEO supramolecular complex in DMF/MeCN solution at a MeCN content of 70 wt%. (b, c) Schematic representation of the possible onion sphere structure observed in the TEM image in (a). (e) Schematic representation of the possible woodlouse structure observed in the TEM image in (d). (f) Size-distributions of the micelles by using DLS, corresponding to the TEM images in (a) and (d).

Polymer Chemistry Accepted Manuscript

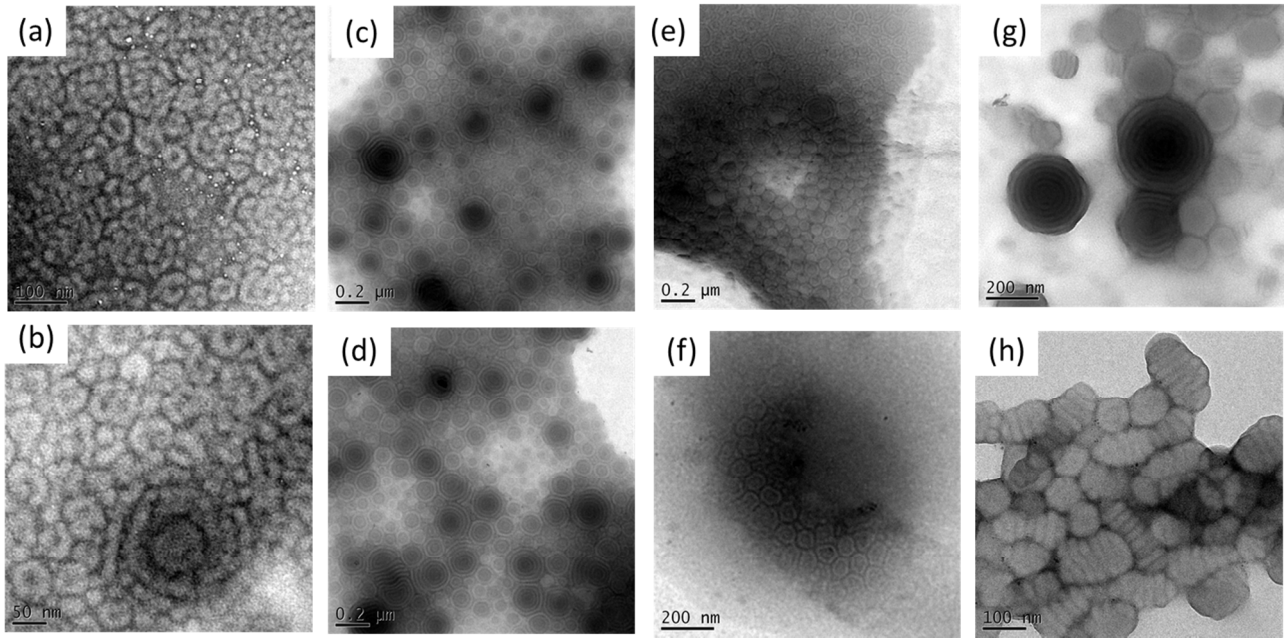

Figure 10: TEM images of PS_{87}-*b*-$PVBT_{22}$/A-PEO supramolecular complexes formed in DMF/MeCN solution at a MeCN content of 70 wt% at T/A ratios of (a, b) 1:0.3, (c, d) 1:0.5, (e, f) 1:0.7, and (g, h) 1:1.

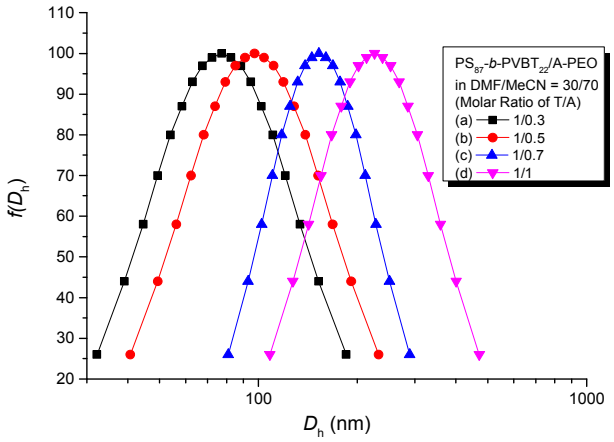

Figure 11: DLS data of PS_{87}-*b*-$PVBT_{22}$/A-PEO supramolecular complexes formed in DMF/MeCN solution at a MeCN content of 70 wt% at T/A ratios of (a) 1:0.3, (b) 1:0.5, (c) 1:0.7, and (d) 1:1.

have received much attention due to their potential application as carriers for controlled-release systems;[44] onion-like morphologies have been reported widely in the bulk state, formed from triblock copolymers, copolymer/homopolymer blends, and copolymer/copolymer blends, where thermodynamic equilibrium plays an important role.[45,46] In this study, we observed onion structures of various sizes and with different numbers of ring patterns [**Figure 9(a)**]. As revealed in **Figure 4**, the vesicle structure arose from the bilayer structure of the supramolecular complex of (PEO-A/PVBT-*b*-PS/PS-*b*-PVBT/A-PEO). At a high MeCN content (70 wt%), the micelle structure was close to precipitating and close to behaving as in the bulk state. Therefore, the double-bilayer structure of (PEO-A/PVBT-*b*-PS/PS-b-PVBT/A-PEO) bent into relatively smaller onion structures, with no MeCN existing inside the micelle structure because of the relatively low interaction parameter ($\chi_{PS\text{-}MeCN}$) did not induce strong segregation between the PS block and MeCN solvent; the triple bilayer structure of (PEO-A/PVBT-*b*-PS/PS-b-PVBT/A-PEO) also bent into relatively larger onion structures [**Figures 9(b)** and **9(c)**]. From these results, we may suspect that these onion structures in this system may have possessed non-equilibrium or kinetically captured morphologies, because the PS and PVBT block segments [with relatively high glass transition temperatures (T_g)] were in the glassy state, with their mobilities decreasing significantly, at this higher MeCN content. Muller *et al.* reported that the poly(butadiene–*b*–*tert*-butyl methacrylate–*b*–*N*-methyl-2-vinylpyridinium) (PB-*b*-PtBMA-*b*-P2VPq) ABC mikotoarm star terpolymer forms a segmented worm–like structure (woodlouse structure); they also observed an onion structure.[14] In our present study, we observed almost the same woodlouse structures at the higher MeCN content. We propose that these woodlouse structures [**Figures 9(d)** and **9(e)**] may have arisen from further microphase separation of the onion structure. To confirm this phenomenon, we controlled the graft density of the A-PEO segment on the PS-*b*-PVBT block segments. The advantage of preparing pseudo A-*b*-(B-*g*-C) terpolymers from this PS-*b*-PVBT/A-PEO supramolecular complex is that we could readily control the grafting density of PEO by blending with different ratios of A-PEO homopolymer—much easier than having to synthesize individual covalently linked A-*b*-B-*g*-C terpolymers.

Figure 10 presents TEM images of the PS_{87}-*b*-$PVBT_{22}$/A-PEO supramolecular complexes formed at various T/A ratios in DMF/MeCN solution at a MeCN content of 70 wt%. We observed short-range-ordered worm-like and spherical structures at a T/A ratio of 1:0.3, as revealed in Figures 10(a) and 10(b), presumably because the relative low A-PEO content did not provide a sufficiently large outer layer to protect from precipitation of the PS-*b*-PVBT block segments while it was difficult to self-assemble into a regular micelle structure. In contrast, increasing the T/A ratio to 1:0.5 [Figures 10(c) and 10(d)] or 1:0.7 [Figures 10(e) and 10(f)], we observed almost-onion structures; thus, increasing the PEO grafting density stabilized and enhanced the regular multi-compartment micelle structures. Similar to the structures in Figures 7(g)–7(i), we

Polymer Chemistry Accepted Manuscript

This journal is © The Royal Society of Chemistry [year]

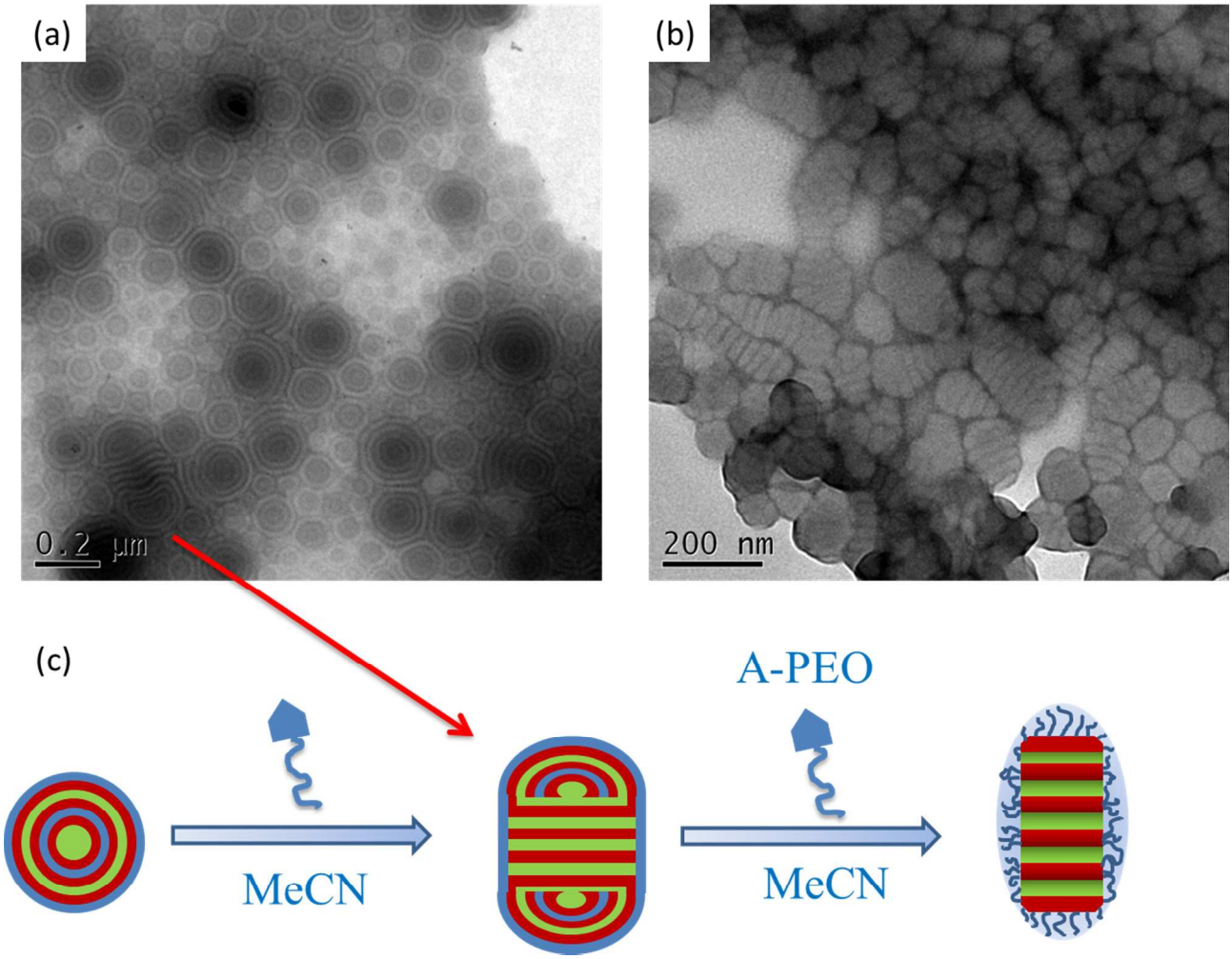

Figure 12: TEM images of PS_{87}-*b*-$PVBT_{22}$/A-PEO supramolecular complexes formed at T/A ratios of (a) 1:0.5 and (b) 1:1. (c) Possible morphologies, from onion structures to woodlouse structures, formed in the DMF/MeCN solution at a MeCN content of 70 wt%.

observed regular woodlouse structures in Figures 10(g) and 10(h) when the T/A ratio was 1:1. In addition, the sizes of micelles increased upon increasing the T/A ratio, as revealed in Figures 10 and 11. Furthermore, the PDI of the values of D_h also increased upon increasing the T/A ratio, because the segmented worm–like structure (woodlouse structure) would increase the PDI of the values of D_h relative to that of the spherical onion structure. More interestingly, we observed an intermediate structure between the onion structure and the woodlouse structure in Figure 12(a) for a T/A ratio of 1:0.5, a segmented woodlouse structure existing between two onion structures. Further increasing the T/A ratio to 1:1, we found almost the same segmented woodlouse structure as that in **Figure 12(b)**. Therefore, increasing the A-PEO grafting density to equal stoichiometry with PVBT led to equilibrium between the segmented worm–like or woodlouse structures in this study.

WAXD Analyses of PS-b-PVBT/A-PEO Supramolecular Complexes

To realize the phase separation and crystallization behavior of the A-PEO segments in the different selective solvents, we prepared thin films of the PS_{87}-*b*-$PVBT_{22}$/A-PEO supramolecular complexes through spin coating onto silicon wafers from DMF/H_2O and DMF/MeCN solutions. **Figure 13** displays the WAXD patterns of the PS_{87}-*b*-$PVBT_{22}$/A-PEO supramolecular complexes. No diffraction peaks were evident for the PS-*b*-PVBT block copolymer in **Figure 13(a)**, as would be expected for the amorphous segments of both the PS and PVBT blocks. For PS-*b*-PVBT/A-PEO mixtures dissolved the common solvent DMF, we observed weak diffraction peaks in **Figure 13(b)**, indicating that the PEO segment could not crystallize by itself because of the high solubility of the PEO segment in the common solvent DMF. In contrast, the addition of a selective solvent, either water or MeCN, caused diffraction peaks to appear, with increased intensity upon increasing the content of the selective solvent [**Figure 13(A)** for water; **Figure 13(B)** for MeCN]. The obvious diffraction peak was corresponding to the (120) plane of the PEO crystallite at a value of 2θ of 19.1°, appeared in the WAXD patterns upon increasing the content of each selective solvent; the similar result has been observed for a pure A-PEO homopolymer.[47] As a result, the addition of a selective solvent into a solution of the PS-*b*-PVBT/A-PEO supramolecular complex could enhance the microphase separation of the A-PEO and PS-*b*-PVBT block copolymer segments, thereby inducing micelle structures in solution. The most important feature was multiple hydrogen bonding between the T groups of PVBT and the A group of A-PEO. We recorded ^{1}H NMR spectra of PT (as a model compound for PVBT) and A-PEO to confirm the presence of

Polymer Chemistry Accepted Manuscript

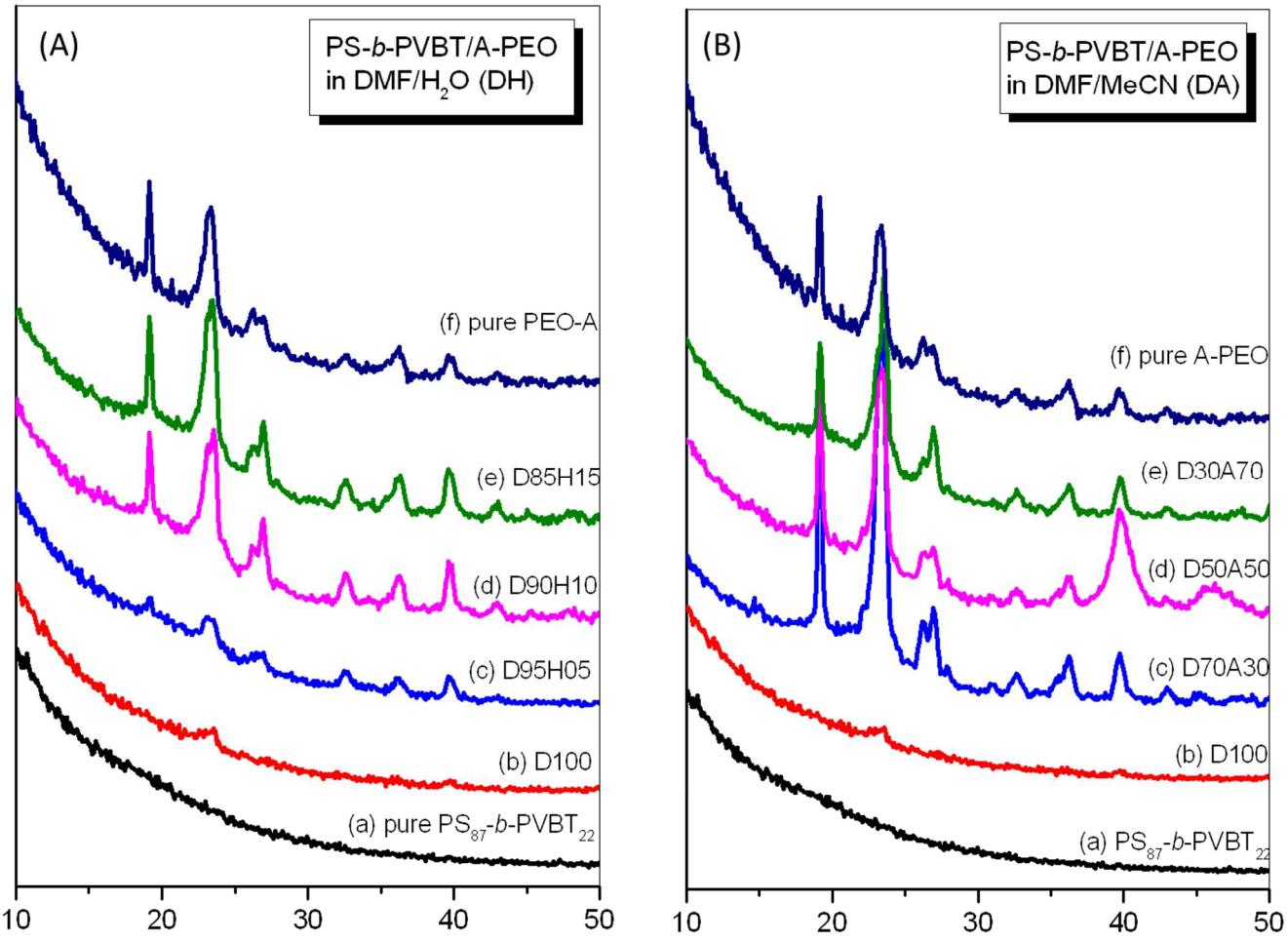

Figure 13: WAXD patterns of PS_{87}-*b*-$PVBT_{22}$/A-PEO supramolecular complexes formed at various contents of the selective solvent: (A) DMF/H_2O and (B) DMF/MeCN solutions.

multiple hydrogen bonding interactions between the T groups of PVBT and the A group of A-PEO (**Figure S4**). The addition of A-PEO to a solution of PT led to a downfield shift of the signal for the NH unit of the T group, appearing initially at 8.40 ppm and moving to 10.38 ppm when the T/A ratio was 1:1.[48,49] Similarly, the addition of PT to a solution of A-PEO resulted in a downfield shift of the signal of the NH_2 unit of the A group, from 5.64 to 6.40 ppm, confirming that multiple intermolecular hydrogen bonding occurred between their T and A groups.

Scheme 2 summarizes the morphologies of the multi-compartment micelles obtained from the PS-*b*-PVBT/A-PEO supramolecular complexes in this study. By varying the molecular weights of the PS-*b*-PVBT block segments and increasing the content of water as the selective solvent, we would change the structures of the multi-compartment micelles from raspberry-like spheres to core–shell–corona cylinders to trilayer vesicles to in-plane multilayer vesicle structures [Schemes 2(a)–2(d)]. Similarly, the multi-compartment micelles changed from core–shell–corona spheres to core–shell–coronal cylinders to onion-like structures to and woodlouse structures upon increasing the content of MeCN [Scheme 2(e)–2(h)]. Through simple blending of the A-PEO homopolymer into the PS-*b*-PVBT block copolymers, we could also observe changes in the structures of the multi-compartment micelles that were similar to those of ABC miktoarm star terpolymers. A further attractive feature of this supramolecular complex is that we could readily control the grafting density of the PEO segment through simple blending with different amounts of the A-PEO homopolymer; in comparison, it is difficult to control the structures of real (i.e., covalent) A-*b*-(B-*g*-C) terpolymers.

Conclusions

We have proposed a simple but effective method for preparing various multi-compartment micelle structures from PS-*b*-PVBT/A-PEO supramolecular complexes, which undergo hierarchical self-assembly through the multiple hydrogen bonding interaction of their T and A units. We grafted A-PEO onto PS-*b*-PVBT diblock copolymers to form pseudo A-*b*-(B-*g*-C) terpolymers stabilized through complementary multiple hydrogen bonding in DMF solution; increasing the content of added water as a selective solvent transformed the morphology from raspberry-like spheres to core–shell–corona cylinders to trilayer vesicles to in-plane multilayer vesicles. Likewise, the the morphologies of the multi-compartment micelles changed from core–shell–corona spheres to core–shell–coronal

Polymer Chemistry Accepted Manuscript

This journal is © The Royal Society of Chemistry [year]

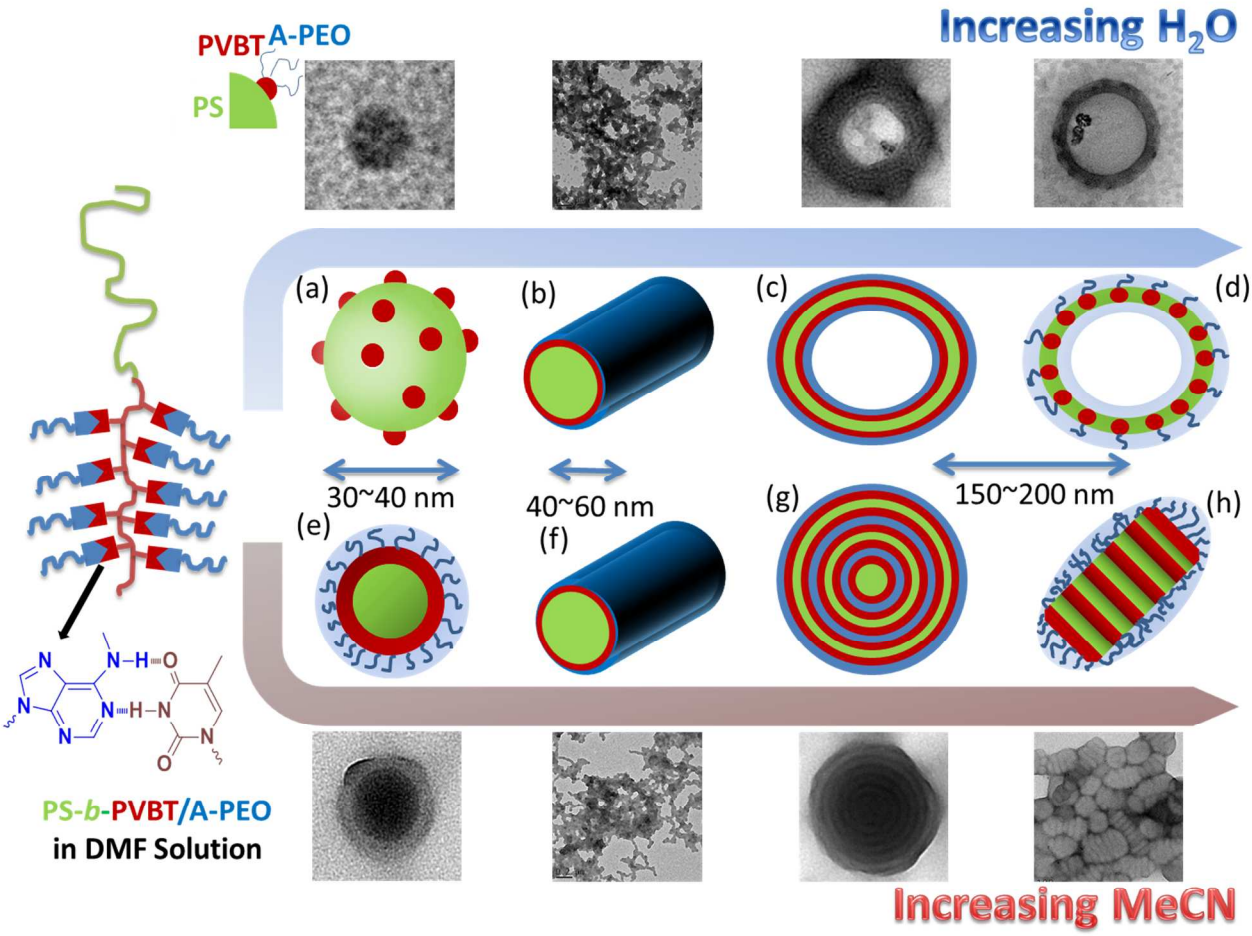

Scheme 2: Changes in the multi-compartment micelle structures of PS-*b*-PVBT/A-PEO supramolecular complexes in DMF solution upon increasing the contents of (a)–(d) H_2O and (e)–(h). MeCN as selective solvents.

cylinders to onion structures to woodlouse structures upon increasing the MeCN content. We are optimistic that this simple method will facilitate the development of various other multi-compartment micelles for biomedical use as well as templates for the synthesis of unprecedented porous inorganic nanomaterials.

Acknowledgment

This study was supported financially by the Ministry of Science and Technology, Republic of China, under contracts MOST 100-2221-E-110-029-MY3 and MOST 102-2221-E-110-008-MY3. Dr. Yi-Chen Wu also thanks 2014 New Partnership Program for the Connection to the Top Labs in the World under contracts MOST 103-2911-I-110-513 that helped initiate this study. We also thank Mr. Hsien-Tsan Lin (Regional Instruments Center at National Sun Yat-Sen University) for his help with TEM experiments.

Electronic supplementary information (ESI) available:

GPC, ^{1}H NMR, SAXS and TEM images of PS-*b*-PVBT diblock copolymer.

Reference

1. L. Zhang, and A. Eisenberg, *J. Am. Chem. Soc.,* 1996, **118**, 3168-3181.
2. A. Halperin, M. Tirrell, and T. P. Lodge, *Adv. Polym. Sci*., 1992, **100**, 31-71.
3. G. Kaur, L. Y. Chang, T. D. M. Bell, T. W. Hearn, and K. Saito, *J. Polym. Sci. Part A: Polym. Chem.,* 2011, **49**, 4121-4128.
4. A. O. Moughton, M. A. Hillmyer, and T. P. Lodge, *Macromolecules,* 2012, **45**, 2-19.
5. S. Kubowicz, J. F. Baussard, J. F.; Lutz, A. F. Thunemann, H. von Berlepsch, and A. Laschewsky, *Angew. Chem., Int. Ed.,* 2005, 44, 5262–5265.
6. H. von Berlepsch, C. Bottcher, K. Skrabania, and A. Laschewsky, *Chem. Commun.,* 2009, **17**, 2290-2292.
7. F. Huo, S. Li, Q. Li, Y. Qu, and W. Zhang, *Macromolecules*, 2014, **47**, 2340-2349.
8. A. Wang, J. Huang, and Y. Yan, *Soft Matt.,* 2014, **10**, 3362-3373.
9. A. H. Groschel, F. H. Schacher, H. Schmalz, O. V. Borisov, E. B. Zhulina, A. Walther, and A. H. E. Muller, *Nature Commun.,* 2012, **3**, 1-10.
10. J. F. Lutz, and A. Laschewsky, *Macromol. Chem. Phys.,* 2005, **206**, 813-817.

Polymer Chemistry Accepted Manuscript

11. A. Laschewsky, *Curr. Opin. Colloid Interface Sci.,* 2003, **8**, 274-281.
12. Z. Li, E. K. Kesselman, Y. Talmon, M. A. Hillmyer, and T. P. Lodge, *Science,* 2004, **306**, 98-101.
13. Z. Li, M. A. Hillmyer, and T. P. Lodge, *Langmuir,* 2006, **22**, 9409-9417.
14. A. Hanisch, A. H. Groschel, M. Fortsch, M. Drechsler, H. Jinnai, T. M. Ruhland, F. H. Schacher, and A. H. E. Muller, *ACS Nano,* 2013, **7**, 4030-4041.
15. W. Wang, J. Zhang, C. Li, P. Huang, S. Gao, S. Han, A. Dong, and D. Kong, *Colloid Surface B: Biointerfaces,* 2014, **115**, 302-309.
16. S. W. Kuo, P. H. Tung, C. L. Lai, K. U. Jeong, and F. C. Chang, *Macromol. Rapid Commun.,* 2008, **29**, 229-233.
17. S. W. Kuo, P. H. Tung, and F. C. Chang, *Eur. Polym. J.,* 2009, **45**, 1924-1935.
18. S. W. Kuo, *Polym. Int.,* 2009, **58**, 455-464.
19. M. R. Talingting, P. Munk, S. E. Webber, and Z. Tuzar, *Macromolecules,* 1999, **32**, 1593–1601.
20. J. Zhu, and R. C. Hayward, *Macromolecules,* 2008, **41**, 7794-7797.
21. Z. Li, M. A. Hillmyer, and T. P. Lodge, *Macromolecules,* 2006, **39**, 765-771.
22. H. G. Cui, Z. Y. Chen, S. Zhong, K. L. Wooley, and D. J. Pochan, *Science,* 2007, **317**, 647-650.
23. Guo, M.; Jiang, M. *Soft Matt.,* 2009, **5**, 495-500.
24. A. O. Moughton, and R. K. O'Reilly, *J. Am. Chem. Soc.,* 2008, **130**, 8714-8725.
25. S. Y. Liu, G. Z. Zhang, and M. Jiang, *Polymer,* 1999, **40**, 5449-5453.
26. H. Kuang, S. Wu, F. Meng, Z. Xie, X. Jiang, and Y. Huang, *J. Mater. Chem.*, 2012, **22**, 24832-24840.
27. X. Y. Hu, T. Xiao, C. Lin, F. Huang, L. Wang, *Acc. Chem. Res.* 2014, **47**, 2041-2051.
28. R. Chakrabarty, P. S. Mukherjee, P. J. Stang, *Chem. Rev.* 2011, **111**, 6810-6918.
29. C. H. Lu, C. F. Huang, S. W. Kuo, and F. C. Chang, *Macromolecules,* 2009, **42**, 1067-1078.
30. Y. C. Wu, and S. W. Kuo, *Polym. Chem.,* 2012, **3**, 3100-3111.
31. Y. R. Wu, Y. C. Wu, and S. W. Kuo, *Macromol. Chem. Phys.,* 2013, **214**, 1496-1503.
32. K. W. Huang, Y. R. Wu, K. U. Jeong, and S. W. Kuo, *Macromol. Rapid Commun.,* 2013, **34**, 1530-1536.
33. Y. C. Wu, Y. S. Wu, and S. W. Kuo, *Macromol. Chem. Phys.,* 2013, **214**, 563-571.
34. L. Zhang, and A. Eisenberg, *Science,* 1995, **268**, 1728-1730.
35. L. Zhang, K. Yu, and A. Eisenberg, *Science,* 1996, **272**, 1777-1779.
36. P. Bhargava, J. X. Zheng, P. Li, R. P. Quirk, F. W. Harris, and S. Z. D. Cheng, *Macromolecules,* 2006, **39**, 4880-4888.
37. P. Bhargava, Y. Tu, J. X. Zheng, H. Xiong, R. P. Quirk, and S. Z. D. Cheng, *J. Am. Chem. Soc.,* 2007, **129**, 1113-1121.
38. Y. Mai, and A. Eisenberg, *Chem. Soc. Rev.,* 2012, **41**, 5969-5985.
39. A. K. Brannan, and F. S. Bates, *Macromolecules,* 2004, **37**, 8816-8819.
40. P. C. Li, Y. C. Lin, M. Chen, and S. W. Kuo, *Soft Matt.,* 2013, **9**, 11257-11269.
41. H. Shen, and A. Eisenberg, *Angew. Chem. Int. Ed.,* 2000, **39**, 3310-3312.
42. L. Lei, J. F. Gohy, N. Willet, J. X. Zhang, S. Varshney, and R. Jerome, *Macromolecules,* 2004, **37**, 1089-1094.
43. J. Ding, and G. Liu, *Macromolecules,* 1999, **32**, 8413-8420.
44. K. Zhang, L. Gao, Y. Chen, and Z. Yang, *J. Coll. Interface Sci.,* 2010, **346**, 48-53.
45. C. W. Chiou, Y. C. Lin, L. Wang, T. Hayakawa, and S. W. Kuo, *Macromolecules,* 2014, **47**, 8709-8721.
46. L. Sun, L. Zhu, L. Rong, and B. S. Hsiao, *Angew. Chem. Int. Ed.,* 2006, **45**, 7373-7376.
47. C. He, J. Sun, J. Ma, X. Chen, and X. Jing, *Biomacromolecules,* 2006, **7**, 3482-3489.
48. S. W. Kuo, and R. S. Cheng, *Polymer,* 2009, **50**, 177-188.
49. Y. C. Wu, and S. W. Kuo, *J. Mater. Chem.,* 2012, **22**, 2982-2991.

Polymer Chemistry Accepted Manuscript

This journal is © The Royal Society of Chemistry [year]

CREATED USING THE RSC ARTICLE TEMPLATE (VER. 3.1) - SEE WWW.RSC.ORG/ELECTRONICFILES FOR DETAILS

A Graphic Content

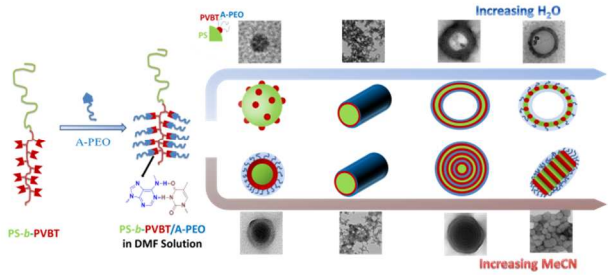

Several different multi-compartment micelle structures: raspberry-like spheres, core–shell–corona spheres, core–shell–corona cylinders, nanostructured vesicles, onion-like structures, segmented worm–like cylinders, and woodlouse-like structures through upon the concentration of the selective solvent.

Polymer Chemistry Accepted Manuscript